CHAPTER-2

Solution-processed, Highly-efficient Organic Field-effect Transistor based Hydrogen Sulfide Gas Sensor at sub-ppm Regime

The part of the work is adopted from-

V. K. Singh, A. Verma, P. Kumar and V. N. Mishra, "Solution-Processed, Highly-Efficient Organic Field-Effect Transistor Based Hydrogen Sulfide Gas Sensor at Sub-ppm Regime," in ***IEEE Sensors Journal,*** vol. 23, no. 15, pp. 16600-16607, 1 Aug.1, 2023, ***doi: 10.1109/JSEN.2023. 3288932.***

Abstract

In regard to take a step closer towards the problem statement identified in Chapter 1, in the current article, we have investigated a highly selective, sensitive, low-power, and cost-efficient H_2S gas sensor utilizing the thin film of conjugated organic polymer Poly[2,6-(4,4-bis-(2-ethylhexyl)-4H-cyclopenta [2,1-b; 3,4-b'] dithiophene)-alt-4,7-(2,1,3-benzothiadiazole)] (PCPDTBT) as an active sensing layer. The organic thin film of PCPDTBT polymer is developed using a cost-effective, facile solution-processed floating film transfer method (FTM). Additionally, state-of-the-art technique used for annealing named 'solvent vapor annealing' offers enhanced crystallinity, excellent charge transfer along the polymer chain which, significantly improves sensitivity. The fabricated organic field effect transistor (OFET) with Top contact bottom gate (TCBG) configuration is thoroughly explored to investigate the thin film's electrical and gas sensing performance for toxic and hazardous H_2S gas. The fabricated device worked at room temperature (RT-25 ºC) and was highly sensitive to the presence of H_2S gas at concentrations even lower than 1 ppm. The fabricated OFET device has excellent air stability, good response–recovery behavior (response/recovery time of 8/250 sec, respectively), exceptional gas response reproducibility, and a high sensor response of 71.3% at 1 ppm H_2S gas exposure.

2.1 Introduction

Hydrogen sulfide (H_2S) is a colorless, highly toxic, corrosive, hazardous, and flammable gas at ambient conditions. According to Occupational Safety and Health Administration (OSHA), after carbon monoxide (CO), hydrogen sulfide (H_2S) is one of the most hazardous chemicals in the workplace [61]. Since H_2S gas is denser than ambient air and can easily accumulate in enclosed spaces at or below ground level, making these

environments highly poisonous, dangerous, and off-limits for work. The toxicity of H_2S strongly depends upon its concentration level and duration of exposure. It is classified into three different categories, (1) acute exposure (greater than 300 ppm), (2) post-acute exposure (greater than 100 ppm); and (3) chronic exposure (less than 10 ppm) [23]. Acute exposure (higher concentration for a short duration) may cause cardiopulmonary paralysis [62], unconsciousness, collapse, and even death over 1000 ppm and higher concentrations [25]. Compared to acute exposure, post-acute exposure occurs over a medium exposure duration, i.e., 30 minutes, and can result in unconsciousness, breathing problems, and other pulmonary disorders. Chronic exposure occurs when less than 10 ppm of hydrogen sulfide gas is exposed over several days, with effects including skin and eye irritation, headache, and nausea [24]. OSHA has established workplace H_2S exposure standard limits, which include an 8-hour exposure restriction of 10 ppm and a 15-minute exposure restriction of 15 ppm [61]. Therefore, in order to meet the demands for extremely effective sensors and reduce the hazardous effects of this dangerous gas, the development of H_2S gas sensors has been continuously improved. Various materials and methods have been employed for H_2S monitoring, including optical, electrochemical, and surface acoustic wave (SAW) techniques [25][22]. Although the fluctuation of the environment would not deteriorate the execution of these methods, their utilization as a gas sensor is severely constrained due to size, comparatively high cost, constrained temperature range, and selectivity. Metal-oxide-semiconductor (MOS)-based sensors are the most extensively utilized gas sensors in recent decades because of their prominent availability and inherent benefits as gas-sensitive materials [52]. In addition to having a restricted selectivity and a significant reliance on relative humidity, MOS-based sensors often require a solid substrate and a higher operational temperature (temp. >100 °C), which restricts their

potential applications in the fields of smart wearable electronics, flexible electronics, and low-power electronic operations. Therefore, it is essential to fabricate low-temperature operated devices along with high sensitivity, fast transient (recovery and response) characteristics, and selectivity for the efficient and safe detection of H_2S during in-situ monitoring to mitigate operational and health hazards. Other benefits of low operating temperature include less power usage, improved long-term stability, and use in self-powered devices. Considering these challenges, using organic semiconducting polymer (OSP) as a sensitized surface, which can address these current limitations, is considered a promising alternative to MOS sensors. OSP materials are interesting category to use in portable, low-cost, room temperature (RT) operable gas sensors. In addition, OSP materials offer the benefits of mechanical flexibility, solution processability, and tailorable chemical properties [63][16]. Recently, "Poly[2,6-(4,4-bis-(2-ethylhexyl)-4H-cyclopenta [2,1-b;3,4-b′]dithiophene)-alt-4,7(2,1,3-benzothiadiazole)]" (PCPDTBT) has emerged as a potential conducting polymer having significant scientific attentions [64]–[67]. PCPDTBT is a copolymer based on cyclopenta dithiophene (CPDT) as the electron donor unit and 2,1,3-benzothiadiazole (BTD) as an electron deficient or withdrawing unit. Both, Dithiophene (DT) and Benzothiadiazole (BTD) functional groups are found sensitive to Hydrogen sulfide gas in the recently published literature [68][69]. Moreover, the development of ordered and self-organized structures with improved charge transfer properties due to the presence of higher-order alkyl side chains and π-π stacking is an additional benefit [64]. However, to the best of our knowledge, no study is available to comment on this organic polymer's gas-sensing performance. That is why we have thoroughly investigated this material's electrical and gas-sensing properties. The current work uses organic FET (field-effect transistor) gas sensor due to their sensitive detection, multiparametric

analysis, and compactness [20]. Also, it is possible to modify the channel conductivity by subjecting the gate electrode to various biasing voltages through a thin oxide layer. Additionally, compared to NH_3 and NO_2, only a small number of works focusing on H_2S sensing using OFETs have been investigated and reported All the points mentioned earlier motivated us to carry out the present study. For the development of a uniform self-aligned thin film of organic polymer on the substrate, a facile and inexpensive technique known as the floating film transfer method (FTM) has been efficiently utilized, as illustrated in **Figure 2.1**. Important considerations for thin film deposition under FTM include the orthogonality of the solvents employed in the preparation of the liquid substrate and the solution of OSPs [44]. A drop of low boiling point polymer solution dropped over an orthogonal liquid substrate (mixtures of glycerol (Gl) and ethylene glycol (Eg)) produces a thin floating film by spreading the polymer solution over the liquid substrate followed by evaporation of the polymer solvent. The molecular orientation of the floating film is provided by multiple processes, like the evaporation of the solvent employed in the polymer solution and the viscous force of the liquid substrate [45]. The film can be transferred to any kind of substrate using a simple stamping method. In the present work, the State-of-the-Art technique called 'Solvent vapor annealing (SVA)' enhances the crystallinity of the organic film, which further improves the π-π stacking of the polymer chain and results in better charge injection and charge transport. Solvent vapor annealing is as an effective and versatile alternative to thermal annealing to equilibrate and control the assembly of polymer chains in thin films. Applying simple thermal treatments above the system's limiting glass transition temperature (Tg) in some systems can help with obtaining the equilibrium structure. However, for many large molar mass systems, heat treatments alone are typically inadequate, demanding exceptionally long annealing times. An

alternative annealing technique called solvent vapor annealing (SVA) has often been shown to be far more effective in overcoming such prolonged annealing durations. In SVA, already-formed polymer thin films are exposed to solvent vapours at temperatures that are typically significantly lower than the bulk Tg of both blocks. This causes a swelling and mobile polymer film to develop on top of the substrate. The subsequent solvent evaporation leads to the formation of more structured polymer chain nanostructures [70]–[73].

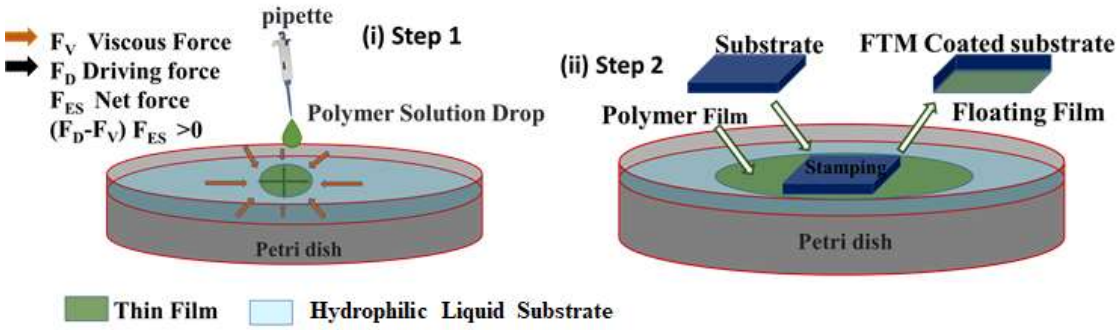

Figure 2.1 (a) Self-alignment of the floating film, (b) Stamping/transfer of the floating film over the ODTS-treated SiO_2 dielectric film.

2.2 Experimental Section

2.2.1. Materials Used

The polymer PCPDTBT (average molecular weight Mw: 7 – 20 kDa) has been purchased from Sigma Aldrich (USA). Highly pure Hydrogen Sulfide gas (99.99%) has been purchased from Sigma Gases and Services Pvt. Ltd. (India). All other chemicals used in the present work were purchased from Merck (India) and used without further processing.

2.2.2. Device Fabrication

The architecture of the fabricated gas sensing device as depicted in **Figure 2.2(a),** is based on an organic semiconducting polymer operating as the active layer in a top-contact, bottom-gate OFET structure.

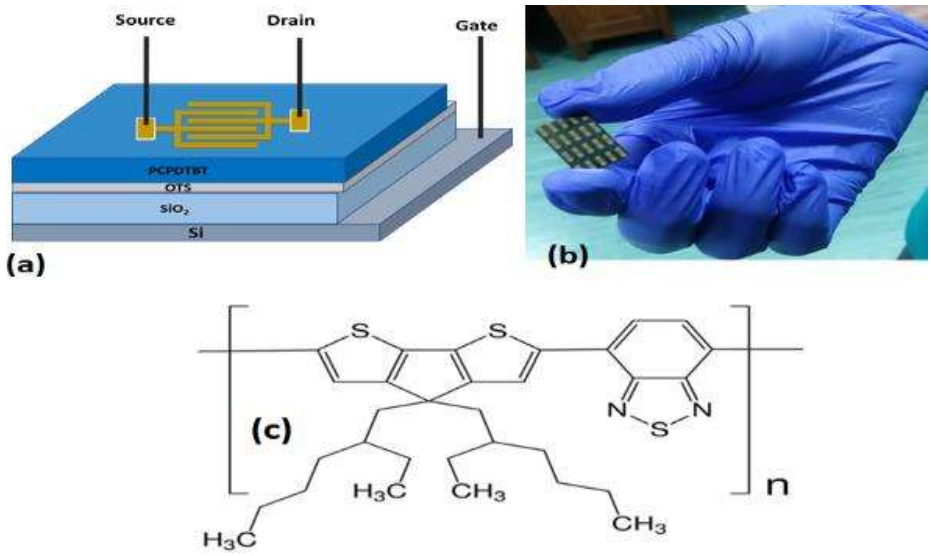

Figure 2.2 (a) Schematic Diagram of the fabricated sensor (b) Device Image (c) Molecular structure of PCPDTBT.

The following procedure has been utilized for the fabrication of the Organic FET. A heavily doped p++ Silicon wafer is cleaned by the standard wet cleaning process. The dry oxidation of the cleaned wafer is carried out to grow 300 nm (measured by Filmetrics F20-UV) SiO_2 (Oxide) film to utilize as an oxide/dielectric layer. The grown oxide has an oxide capacitance of ~10 nF/cm^2. Further, the surface was treated with O_2 (oxygen) plasma for 5 minutes to obtain an activated surface with uniform surface energy. Further, to passivate the activated surface charge trapping sites and to obtain a hydrophobic surface (improves the semiconducting film adhesion), surface treatment of the Si/SiO_2 wafer was performed using octadecyl trichlorosilane solution (ODTS) (~5 nm monolayer). The thermally grown Si/SiO_2 was dipped for 12 hrs. in 1 mM ODTS solution in toluene and subsequently washed with toluene several times and dried. A drop of the polymer solution (10 mg/ml in chloroform) was dispensed on an Eg: Gl (3:1) mixture (liquid substrate of hydrophilic nature). This combination was selected since it has been observed that this concentration produces films with the highest anisotropy [74]. Dynamic evaporation of

the solvent (chloroform) over the liquid substrate developed a long floating thin film, as shown in **Figure 2.1**(b).

The oriented region of this film was recognized using a polarizer sheet and stamped onto the ODTS-treated Si/SiO_2 substrate. In an Argon glove box, the samples were annealed at 70°C for 30 min. Further, we used Chlorobenzene (CB) vapor to anneal the film for 1 hr. (solvent vapor annealing). The FTM deposited substrate was placed in a closed container which contains an inlet with an opening and closing valve. Another airtight container with chlorobenzene solvent was heated until it produced vapors at a nearly constant rate. Then with the help of an airtight pipe, vapors of chlorobenzene were passed to the inlet of the substrate container for 1 hr. Afterward, thermally evaporated, 50 nm thick gold (Au) drain and source electrodes were deposited by HHV 12A4D thermal coating unit at a constant pressure of $\sim 10^{-6}$ torr.

2.2.3. Thin Film Surface Morphology

Atomic force microscopy (NT-MDT, Model - NTEGRA Prima) was used to evaluate the surface topology and root mean square (RMS) roughness of the deposited polymer thin film in tapping mode configuration. 2-D, 3-D, and Grain analysis AFM images of the solvent vapor annealed and thermally annealed PCPDTBT thin film scanned over a 5×5 μm^2 area in tapping mode configuration are shown in **Figure 2.3** ((a)-(c)) and **Figure 2.3** ((d)-(f)), respectively.

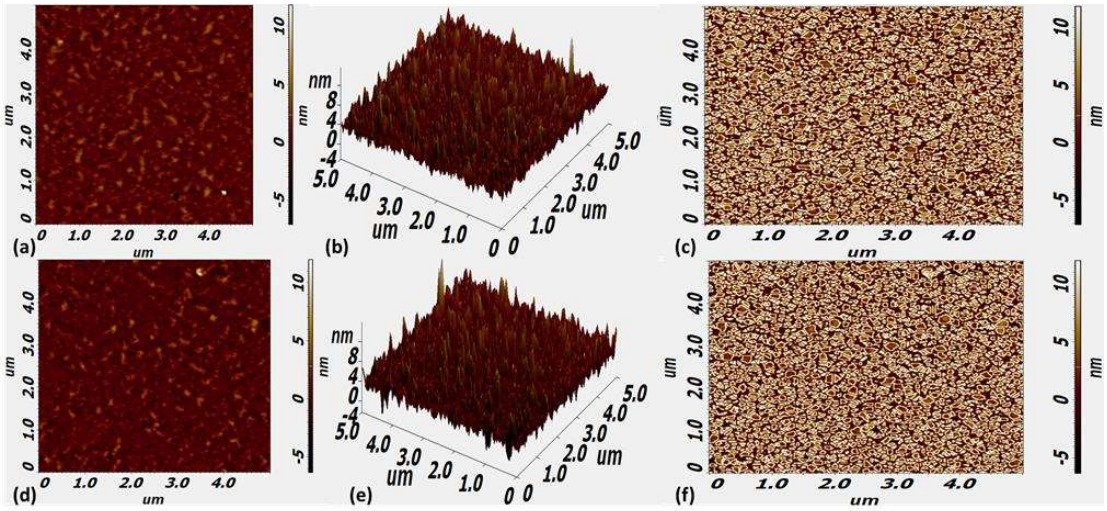

Figure 2.3 2-D, 3-D, and Grain analysis AFM image of the ((a–(c)) Solvent vapor annealed PCPDTBT film and ((d)–(f)) Thermally annealed PCPDTBT film, respectively.

All the extracted parameters are presented in **Table 2.1**. We can observe that the grain size and length has been decreased significantly for the SVA-treated film, while the RMS roughness is slightly higher. The grain analysis of the polymer film presented in **Figure 2.3 (c)** and **Figure 2.3 (f)** demonstrates that the SVA-treated film has developed a large number of grain boundaries compared to thermally annealed film due to decreased grain size. Furthermore, from **Figure 2.3 (a), (c), (d), and (f),** we can observe that the SVA-treated film is slightly better aligned and offers better connected grains. As shown in **Figure 2.3(c),** the interconnected neighboring grains provide a better percolation path for the charge transfer along the active sensing film and enhance the charge transport process [75]. The number of grain boundaries and surface roughness are crucial parameters for the enhanced gas adsorption (physisorption) process. Also, the aligned nature of the film and well-connected grains are crucial for a better charge transport process. As described earlier, the parameters mentioned above have been improved significantly, thus improving the physisorption and charge transport process and enhancing sensitivity. All the improvements discussed in surface morphology are due to the combined effect of the

floating film transfer deposition and solvent vapor annealing method.

Table 2.1 AFM Parameters for SVA and Thermally annealed PCPDTBT film.

Parameters	SVA film	Thermally annealed film
RMS roughness (nm)	2	1.8
Average grain size (nm)	71	82
Average grain length (nm)	110	125

Additionally, we have optimized the thickness of the polymer film by varying the concentration of the polymer solution, composition and temperature of the liquid substrate. Firstly, we observed that decreasing the thickness increases the sensitivity to certain film thicknesses and then starts decreasing. This observed phenomenon is in accordance with the published literature [68]. The optimized film thickness of ~20 nm was measured by Filmetrics F20-UV and also verified by AFM. To measure the thickness of a thin film using an Atomic Force Microscope (AFM), we have used a technique called "step height calibration". First, we used a substrate sample (Si/SiO_2/ODTS) with a known step height, such as a calibration standard. Then, we have scanned the substrate sample with the AFM and measured the height of the step. By comparing the measured height with the known step height, we have calibrated the AFM and determined its sensitivity to height changes. Next, we have scanned our thin film sample (Si/SiO_2/ODTS/PCPDTBT) and measured the height difference between the top surface of the film and the substrate. By multiplying the measured height difference by the sensitivity of the AFM, we have calculated the thickness of the thin film.

2.2.4. Gas Sensing Setup

An indigenous gas-sensing system was built to enable the user to alter experimental settings and meet specific measurement requirements, as shown in **Figure 2.4**. The system included a detection chamber for the gas sensing process, sample/analyte gas (H_2S), dry

air (N_2(79%) and O_2(21%)) for dilution of sample/analyte gas (H_2S), a mass flow controller for controlling dilution and analyte gas, a pneumatic valve for opening and closing gas flow, and a rotary pump for purging the ambient after gas-sensing. The sample gas concentration was adjusted by varying the dilution and analyte gas flow rate during the sensing studies. The fabricated sensor was placed in the detection chamber for gas sensing. Analyte concentrations of 0.2, 0.3, 0.4, 0.5, 0.6, 0.7, 0.8, 0.9, and 1 ppm were used in the experiment. All studies were carried out at RT, 55% RH, under ambient conditions.

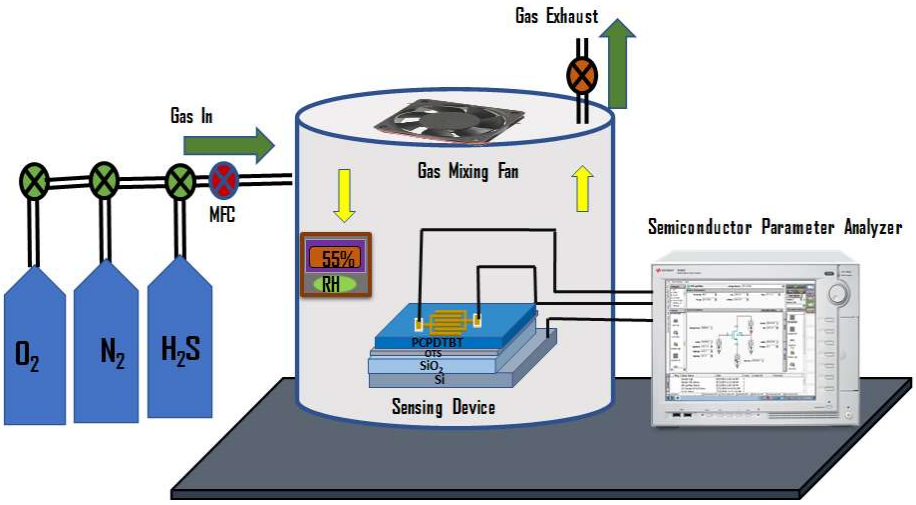

Figure 2.4 Gas Sensing Setup.

2.3 Results and Discussion

2.3.1. Electrical Properties

Electrical characterization of the fabricated OFET device was performed using Agilent KEYSIGHT- B1500 semiconductor parameter analyzer, and the performance of the device was assessed with transfer and output/drain characteristics. Some essential transistor parameters, such as charge carrier mobility (μ_p) and threshold voltage (V_{TH}) were taken into consideration from these behavioral curves to assess the electrical parameters of the fabricated OFET device. The transfer characteristics of the device is plotted by changing the source- drain voltage in fixed steps (0 to -40 V with a step size of 8) while sweeping

the gate-source voltage (V_{GS} = 0 V to -40 V) as depicted in **Figure 2.5(b).** In same manner, the output characteristics of the OFET is plotted by varying source- drain voltage (V_{DS} = 0 V to -40 V) for a fixed gate to source voltages (0 to -40 V with a step size of 8).**Figure 2.5(a)** shows the output/drain characteristics plot of the fabricated organic FET. The following equation was used to get the drain current (I_{DS}) of the OFET in the saturation regime [76]-

$$I_{DS} = \frac{1}{2}\mu_P C_{OX}\frac{W}{L}(V_{GS} - V_{TH})^2 \; ; \; V_{DS} \geq V_{GS} - V_{TH} \quad \textbf{(2.1)}$$

Where μ_P, $C_{OX,}$ W/L, and V_{TH} represent the mobility, capacitance per unit area of the dielectric layer, aspect ratio (AR) of the channel, and threshold voltage respectively**. Equation (2.1)** can be rewritten as:

$$\sqrt{I_{DS}} = \sqrt{\frac{1}{2}\mu_P C_{OX}\frac{W}{L}}(V_{GS} - V_{TH}) = XV_{GS} - Y \quad \textbf{(2.2)}$$

Threshold voltage and mobility are extracted graphically using the linear fitting of **Equation**

(2.2), where Y and X are the intercept and slope, respectively. The mobility and threshold voltage of the OFET can be obtained by **Equation (2.3)** as-

$$\mu_P = \frac{2}{AR.C_{OX}}X^2 \;\&\; V_{TH} = \frac{-Y}{X} \quad \textbf{(2.3)}$$

The trap charge carrier density (Δn_{trap}) of the semiconducting film and dielectric interface can be given by [76]-

$$\Delta n_{trap} = \frac{Q_{trap}}{q} = \frac{\Delta V_{TH} C_{OX}}{q} \quad \textbf{(2.4)}$$

Here Q_{trap} denotes the charge trapped at the semiconductor dielectric interface.

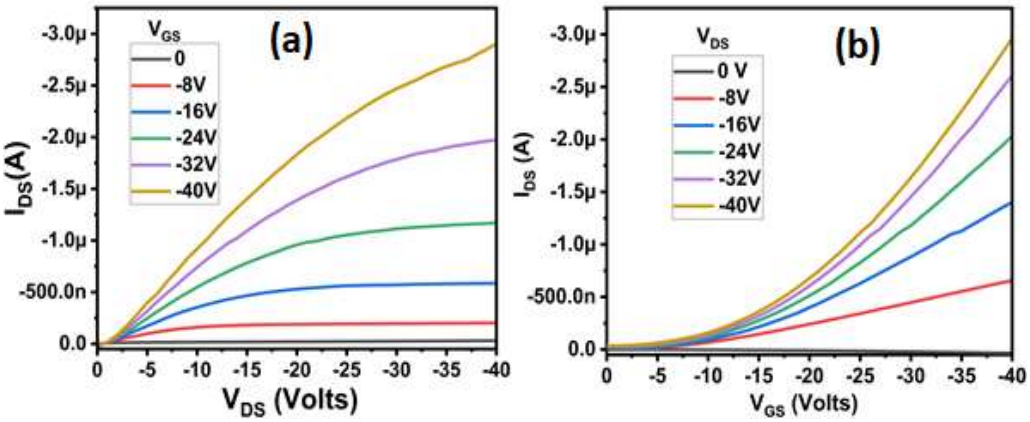

Figure 2.5 (a) Drain characteristics, (b) Transfer characteristics of the fabricated OFET.

It can be observed that the V_{TH} increases with increasing H_2S gas concentration because H_2S molecules have a strong reducing tendency (due to the two lone pair of e^-) and interact with the e^- deficient sites of the PCPDTBT film to form some temporary chemical species in the semiconducting channel layer, which causes modulation in the active charge carrier density in the channel and drain current of the organic FET. The variation in the analyte concentration over the sensing surface results in a notable shift in the fabricated device's threshold voltage (V_{TH}), which is further validated by the mathematical relation expressed by **Equation (2.4**). The charge carrier mobility behavior observation, which shows a dramatic reduction with increasing gas concentration, provided additional confirmation of this phenomenon (**Figure 2.6(b)).** All the extracted electrical and gas sensing parameters upon exposure towards various concentrations of the H_2S gas are tabulated in **Table 2.2.**

2.4 Gas Sensing Properties

2.4.1. Sensor Response

All the measurements were performed at room temperature and ambient environment. The device was subjected to varied gas concentrations of hydrogen sulfide gas, and the corresponding transfer characteristic was reported at V_{GS} = -40 V and V_{DS} = -40 V biasing

condition. The drain current (I_{DS}) change in the transfer characteristics (**Figure 2.6(a)**) is utilized to extract the gas sensor response of the fabricated device at a particular H_2S gas concentration. The sensor response of the device plotted for various concentrations of H_2S gas is depicted in **Figure 2.6(b).** Sensor response has been calculated using [77] –

$$S\% = \frac{\left|I_{DS(AIR)} - I_{DS(GAS)}\right|}{I_{DS(AIR)}} * 100\% \quad \textbf{(2.5)}$$

Unprecedented changes were observed by the OFET device, which exhibited a sensor response of about 71.3% at 1 ppm.

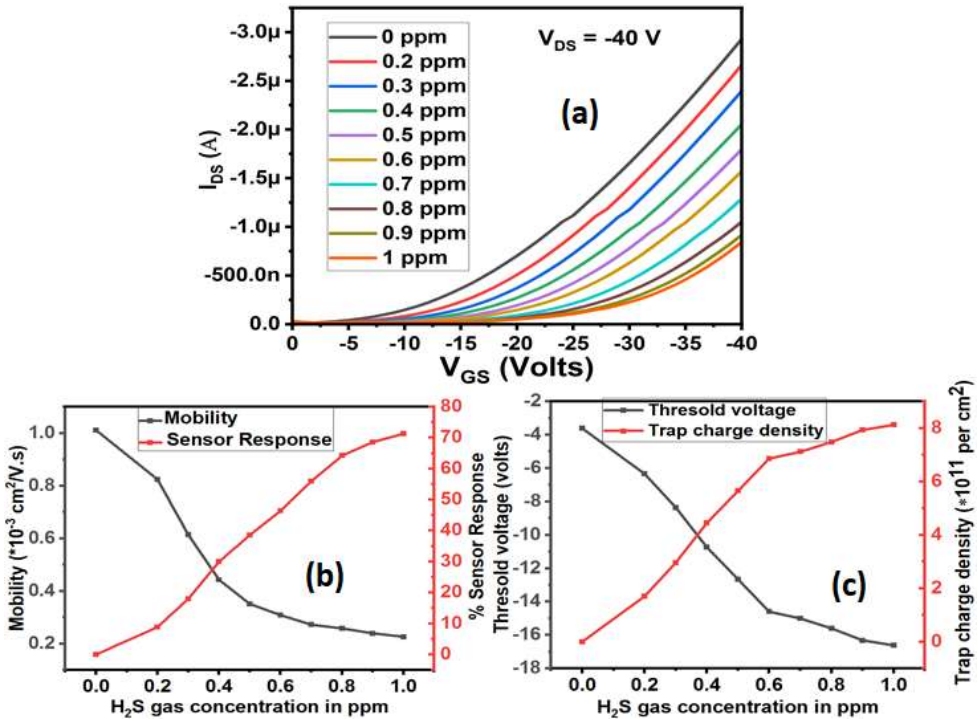

Figure 2.6 (a) The OFET sensor's transfer characteristics at varying H_2S concentrations at V_{DS} = -40 V, (b) Mobility and Sensor Response variation with various H_2S gas concentrations, (c) Threshold Voltage and Trap charge density variation with various H_2S gas concentrations.

Table 2.2 OTFT parameters with exposed H_2S gas.

H_2S ppm	V_{th} (Volts)	Mobility $*10^{-3}(cm^2/V.s)$	Trap density $(*10^{11}/cm^2)$	I_{DS} (µA)	S (%)
0	-3.62	1.01129	0	2.93	0
0.2	-6.34	0.824	1.70	2.67	8.9
0.3	-8.36	0.61377	2.96	2.40	18
0.4	-10.74	0.44272	4.45	2.05	30

0.5	-12.66	0.35099	5.65	1.80	38.6
0.6	-14.60	0.30866	6.86	1.57	46.4
0.7	-15.00	0.27223	7.11	1.29	56
0.8	-15.60	0.25802	7.48	1.05	64.2
0.9	-16.31	0.23927	7.93	0.92	68.6
1	-16.61	0.22645	8.12	0.84	71.3

2.4.2. Transient Analysis and Repeatability

Transient and Stability analysis investigations were carried out to comment on its long-term stability, response-recovery behavior, and repeatability of the device in relation to exposed H_2S gas. It has been observed that when the gas ambient has been removed, the device completely recovers back to the baseline level within a specific time interval.

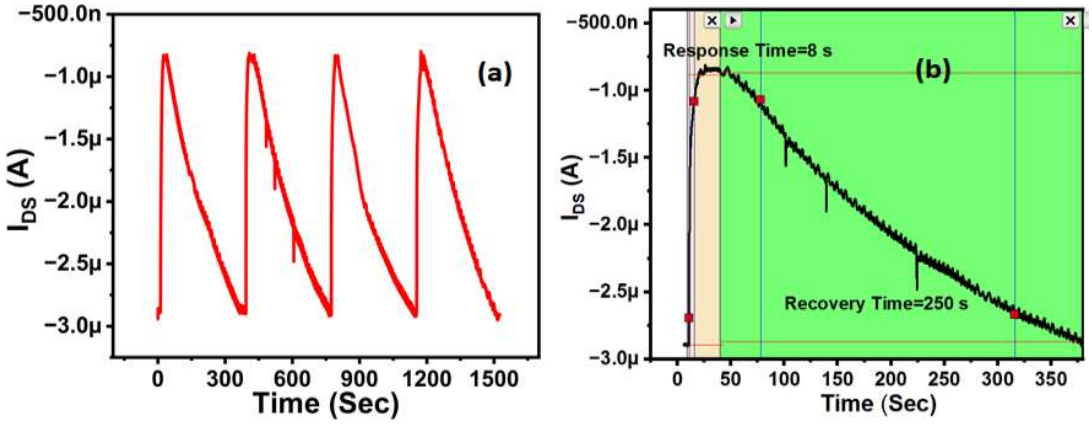

Figure 2.7 (a) Repetitive Transient characteristics of the device at 1 ppm H_2S gas with four consecutive cycles, (b) Zoomed-in image of one transient cycle for response and recovery time analysis.

The repetitive transient response of the sensing device for 4 consecutive cycles is illustrated in **Figure 2.7(a),** demonstrating that the device exhibits excellent repeatability and offers good response-recovery behavior towards the H_2S analyte while keeping the sensor response almost uniform. An extended zoomed-in response/recovery plot for one cycle, as depicted in **Figure 2.7(b),** demonstrate that the device has a response/recovery time of 8/250 sec, respectively, over 1 ppm exposure of H_2S analyte.

2.4.3. Selectivity

The sensor's selectivity was also tested by exposing the device to a variety of interfering gases, such as H_2S, H_2, NH_3, CO_2, CO, and SO_2, at 1 ppm concentration for H_2S and 10 ppm concentration for other gases.

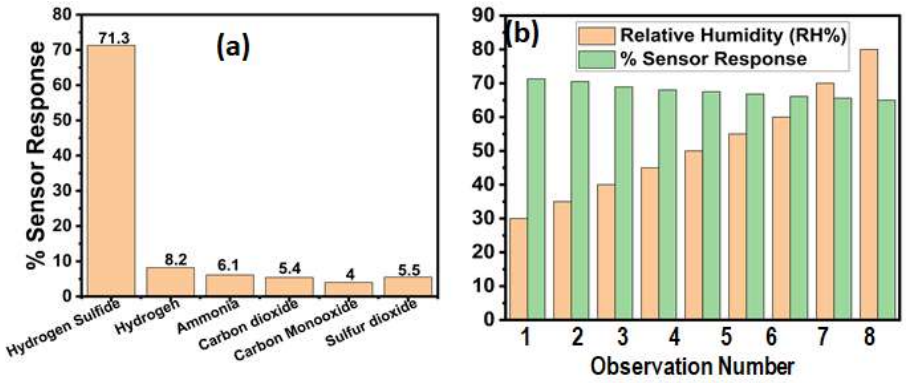

Figure 2.8 (a) Selectivity analysis (b) Relative Humidity analysis.

In **Figure 2.8(a),** the plotted selectivity data demonstrate that the sensor's response to H_2S is considerably higher than the other test gases, demonstrating its exceptional selectivity for H_2S detection. We have observed the response of the ammonia up to 100 ppm concentration, and observed a sensing response of around 55% at 100 ppm. At higher concentrations the sensing response of the sensor is quite significant for ammonia gas but at lower concentration at sub-ppm level, it has highest response and excellent selectivity for hydrogen sulfide gas. This observed phenomenon is consistent with various reports in the literature [68]. The possible reason for the excellent selectivity at lower concentration for hydrogen sulfide gas may be the strong interaction (similar atoms sulfur-sulfur interaction) of the gas with the PCPDTBT as explained in the mechanism section. Further studies are needed to investigate this phenomenon.

2.4.4. Relative Humidity and Stability

The impact of varied humidity (RH%) investigation on the device's current response with H_2S gas exposure is plotted in the bar chart as shown in **Figure 2.8(b)**. Over the range of

30-80% relative humidity (RH) at 1 ppm of exposed H_2S gas, the effect of RH on the sensitivity of the fabricated sensor was investigated. The sensor exhibits almost stable performance over this range. However, at higher relative humidity levels, there was a slight decline in the sensitivity of the fabricated device, probably due to the adsorption of water vapor molecules onto the PCPDTBT sensing film [78]. The adsorption of water vapor molecules reduces the number of vacant sites for analyte adsorption, which reduces the film's sensitivity toward the exposed analyte. Subsequently, a further assessment of the sensor's long-term stability was performed by measuring the drain current degradation (without gas exposure) and sensor response variation (at 1 ppm H_2S analyte) in the ambient conditions (RT with 55% RH) for 8 weeks. Results plotted in **Figure 2.9(b)** illustrate that the sensor offered excellent stability with a minimal percentage degradation of around 7 % and 4.5 % for drain current and sensor response, respectively.

2.4.1. Linearity Analysis

Figure 2.9(a) displays the sensor response plot with different H_2S concentrations at $V_{DS} = V_{GS} = -40$ V. The plot's high correlation coefficient of $R^2 = 0.997$ in region 1 and 0.989 in region 2 demonstrates that the OFET device passes with an excellent linear response for a range of H_2S gas concentrations.

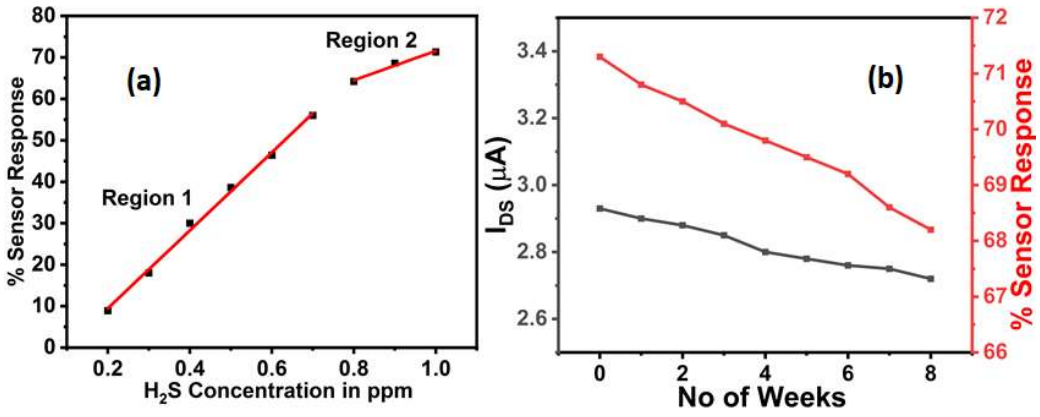

Figure 2.9 (a) Linearity analysis of the sensor (b) Drain current and sensor response change over the weeks.

2.5 Gas Sensing Mechanism

The sensing capabilities of an organic thin film can be affected by a variety of parameters, including the molecular structure of the organic semiconductor, the degree of aligned nature of the film, functional groups present in the polymer, film thickness, surface morphology of the organic film, and the organic film's grain boundaries [21], [68], [79], [80]. As explained in previous sections, all the above parameters have been improved significantly and contribute towards enhanced sensing performance. Furthermore, the gas sensing mechanism can be described in two steps; charge injection (adsorption or physisorption) and charge transport. The physisorption phenomena can be used to describe the dynamic interaction process between PCPDTBT film and H_2S gas. The H_2S molecules participate in the charge transfer interaction as an π electron donor because it is a well-known reductive gas. PCPDTBT is a p-type organic semiconductor whose majority carrier is the hole. H_2S molecules that have been adsorbed on the PCPDTBT film's active adsorption sites and between the grain boundaries inject electrons to PCPDTBT. These injected electrons by H_2S molecules interact with the majority of holes in PCPDTBT film and trap the majority charge carriers of the sensing film. As a result, carrier density and drain current are reduced, and this phenomenon is called 'charge trapping' in the organic polymer sensing film. I_{DS} tends to stabilize once the number of H_2S molecules adsorbed on the PCPDTBT surface is reached at saturation due to unavailability of vacant adsorption sites. The adsorbed H_2S molecules are gradually desorped when the sensing material is exposed to air again or the gas ambiance removed, thus increasing the I_{DS}. After desorption of H_2S molecules from the sensing film, I_{DS} slowly recovers back towards the baseline level.

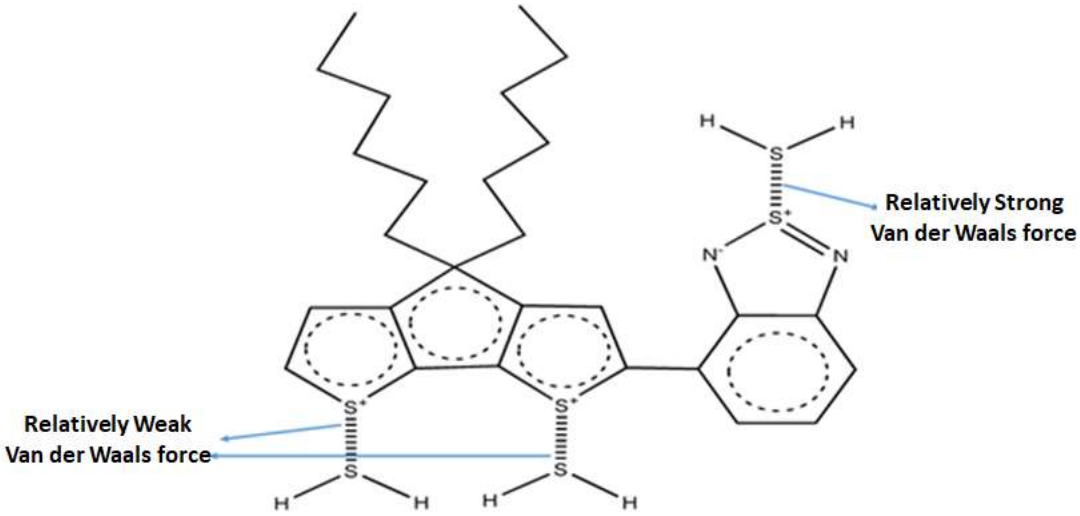

Figure 2.10 H_2S interaction Mechanism With PCPDTBT.

Now we will describe the gas adsorption and charge transport mechanism in detail. As mentioned earlier, both DT and BTD functional groups are found sensitive to hydrogen sulfide gas in recently published literature [68][69]. A possible adsorption mechanism for both the functional groups and combinedly for the PCPDTBT polymer can be seen in the **Figure 2.10**.

BTD functional groups could be employed as units of electron acceptors for conducting materials due to their significant electron-withdrawing ability [81]. BTD is a well-known good electron accepting unit because it contains two electron-withdrawing imine nitrogen atoms (C=N). Also, nitrogen has a much higher electronegativity than sulfur. Therefore, sulfur will be electron deficient and develop a partial negative charge. Thus, the lone pairs of hydrogen sulfide gas will get attached to the sulfur atom of the BTD functional group via a strong van der Waals force. In the case of CPDT, although it is an electron donor group but due to slightly more electronegativity of carbon atom than sulfur, the sulfur atom will develop a much lower partial negative charge compared to the sulfur of the BTD group. Therefore, the lone pairs of hydrogen sulfide gas will get attached to the

sulfur atom of the CPDT functional group via weak van der Waals force. These adsorbed/injected electrons will trap the holes of the PCPDTBT. In addition, due to higher planarity, enhanced conjugation, and stronger intermolecular interactions present in copolymers based on the cyclopenta dithiophene (CPDT) and benzothiadiazole (BTD) will result in better charge carrier transport along the polymer backbone [82].

Charge transport along the PCPDTBT film takes place via the conductive paths formed by the mutually overlapping π orbits of the PCPDTBT rings. The charge transport process can be described with the help of intrachain and interchain transport [75]. The polymer film can be represented as the matrix of connected individual polymer chains. Charge transport occurs dominantly due to intrachain process. Interchain transport occur in the regions where the polymer chains are disordered.

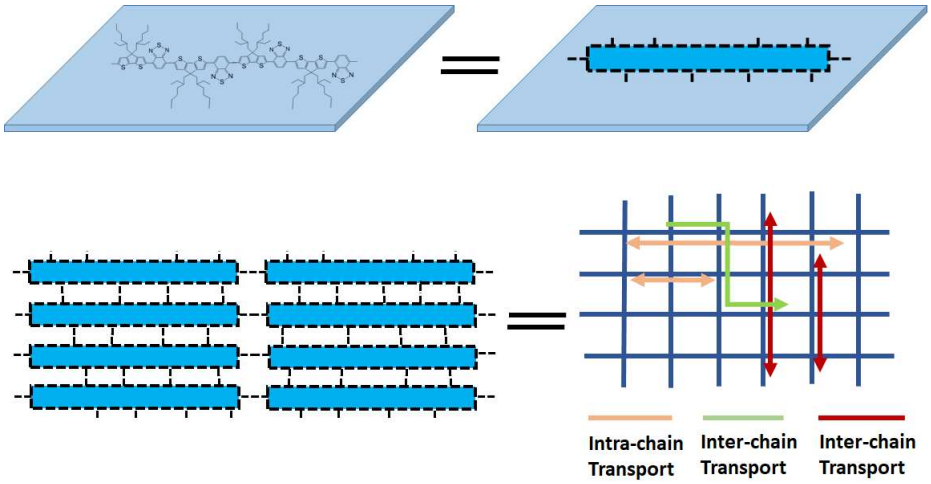

Figure 2.11 Charge Transport Mechanism in Polymer backbone.

We can see the intrachain and interchain transport mechanism in the **Figure 2.11**. Straight tie chain intercrystallite connections (high order alkyl side chains to connect two polymer chains, also called interchain coupling) are expected to promote the high mobility over

the extended backbone of polymer chains from crystallite to crystallite. In case of, presence of disordered regions and amorphous phases surrounding the crystallite domains, high amount of interchain packing supports conjugated polymers for charge carrier localization via interchain transport process [75]. The room temperature operation is possible because the electrical properties of conducting polymers strongly depend on their doping levels. Fortunately, the doping levels of conducting polymers can be easily changed by chemical reactions with many analytes at room temperature (RT), and this provides a simple technique to detect the analytes at RT because the π-conjugation along the polymer chain allows the formation of delocalized electrons via intermolecular conjugated π-bonds, which makes the conducting channel highly sensitive to external analytes at RT [16][22][83].

2.6 Conclusion

In summary, the device offers excellent sensing response, repeatability, response-recovery behavior, and stability against ambient and humidity conditions. The floating film transfer method offers various advantages, i.e., low-cost, solution processibility, large area fabrication, self-alignment of the film, better film morphology, and excellent charge transport, incorporating an enhanced sensing response of the fabricated sensor. Moreover, the solvent vapor annealing process offers enhanced crystallinity, excellent charge injection, and a charge transfer mechanism along the polymer chain, which improves the response/recovery characteristics of the fabricated device. The fabricated sensor exhibits a good sensing response of ~71%, a response/recovery time of 8/250 sec. over 1 ppm exposure of H_2S gas, and is almost independent of relative humidity variation with good ambient stability. Utilizing the developed OFET as an H_2S sensor in actual gas monitoring systems facilitates an exceptional combination of the sensor's high sensitivity,

repeatability, rapid response, and complete recovery after removing the gas ambiance. In summary, the fabricated sensor can be utilized in low-cost, high-performance H_2S gas sensing applications in real-time with sub-ppm range detection capability.